

## A Hybrid Reconfigurable Printed Antenna with Frequency and Pattern

Xinyu Ding, Siwei Li

School of Automation, Chongqing University of Posts and Telecommunications, Chongqing  
400065, China.

dxycqpt@163.com

### Abstract

**A frequency and pattern hybrid reconfigurable WLAN antenna based on structural synthesis is designed. The antenna combines a monopole antenna, a microstrip patch antenna, and a microstrip Yagi antenna. In order to realize the conversion between a total of seven states in the three modes, the PIN diode is used. Simulation and physical test results show that the antenna exhibits omnidirectional radiation characteristics in 2.4GHz monopole mode, and directional radiation characteristics in both 2.4/5.2GHz and 2.4/5.8GHz microstrip patch modes. In these two modes, the antenna has good bandwidth, impedance matching and gain characteristics. In addition, in the two modes of pattern reconstruction, the radiation direction can be changed in a larger angle. The antenna can completely cover the entire frequency range of the WLAN, and its radiation performance can also meet the requirements of WLAN applications.**

### Keywords

**Structural synthesis, Mixed reconfigurable, Printed antenna, PIN diodes.**

### 1. Introduction

The reconfigurable antenna realizes the change of its radiation characteristics through the change of its own structure or the change of the feeding network. It has high adaptability and can improve the performance limitation of the traditional fixed antenna. Therefore, it has been widely studied by scholars at home and abroad.

The research of reconfigurable antennas includes the reconfiguration of frequency, polarization and pattern, and any combination of these three reconfigurable types. Literature [1] provides a butterfly frequency reconfigurable antenna with a novel structure. This antenna can control all PIN diodes through two bias lines to switch the antenna between Bluetooth, WiMAX and WLAN frequency bands. In [2], four PIN diodes and multiple short-circuit posts at 45° intervals are loaded on the center-fed circular patch antenna to achieve linear polarization reconfigurable characteristics. The more common composite reconfigurable antennas include frequency and polarization reconfigurable antennas [3-5], frequency and pattern reconfigurable antennas [6-7], polarization and pattern reconfigurable antennas [8-9].

The reconfigurable antenna changes its radiation characteristics through changes in its structure or feed network. Because of its high adaptability and the ability to improve the performance limitations of traditional fixed antennas, many researchers have paid a lot of attention. However, the reconfiguration of frequency and pattern is mostly limited to traditional design methods, such as parasitic stub loading and tuning, switching feeder networks to select different radiators, etc. There is no systematic design method to guide the rapid design of reconfigurable antennas. Moreover, there are few researches on reconfigurable antennas with multi-band patterns, and reconfigurable antennas with diversified frequencies and patterns are in urgent need of further research.

In view of the above problems, this paper adopts the idea of structural synthesis method. By fusing basic types of monopole antennas, microstrip patch antennas, and microstrip Yagi antennas, a reconfigurable antenna with mixed frequency and pattern is designed. And carried out relevant

theoretical analysis, electromagnetic simulation and test verification, the design method adopted in this paper can provide reference for the design of other reconfigurable antennas.

## 2. Antenna design analysis

The antenna is mainly composed of a rectangular monopole unit on the bottom layer and a metal ground, a microstrip patch unit on the top layer and six metal patches that can function as reflectors/directors. The structure of the antenna and the definition of each parameter are shown in Figure 1. The relative dielectric constant of the antenna dielectric plate  $\epsilon_r$  is 4.4, the size of the dielectric plate is 50mm 50mm, the thickness  $h$  is 1.6mm, and the loss tangent value  $\tan \delta$  is 0.02.

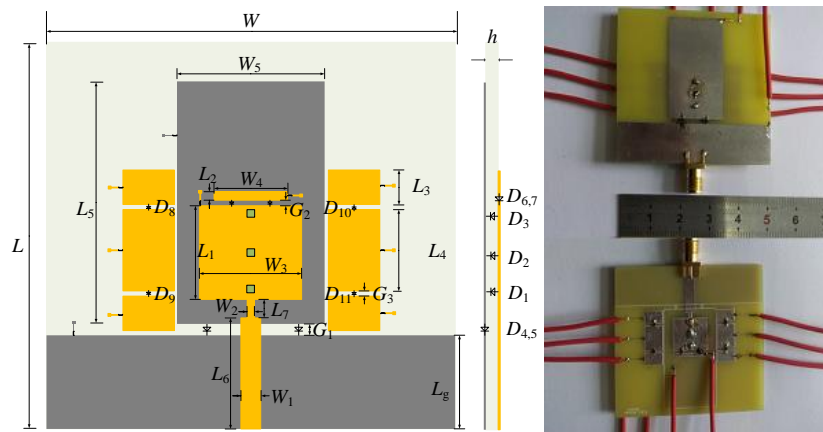


Fig. 1 Schematic diagram of antenna structure and actual antenna

The bottom rectangular monopole unit is used to generate the 2.4GHz resonance frequency band. There is a gap with a width of  $G_1$  between it and the metal ground. When the antenna structure shown in Figure 1 works at 2.4 GHz, its equivalent structure is shown in Figure 2 Mode 1.

The microstrip patch unit on the top layer is mainly used to generate 5.2 GHz and 5.8 GHz resonant frequency bands, which are connected to a 50 ohm microstrip feeder through a stepped impedance transformation section to feed the microstrip patch. The equivalent structure of the antenna when operating at 5.2GHz and 5.8GHz is shown in Figure 2 Mode 2 and Mode 3.

The six-segment metal patch on the top layer is mainly used to act as a director and inverter similar to the Yagi antenna, so as to realize the reconstruction of the pattern of the patch pattern. A DC bias line with a width of 0.2mm is placed vertically on each unit to reduce its impact on the antenna radiation performance. And all DC bias lines are connected to the controlled unit through a 100nH inductance (as a radio frequency choke) to achieve the isolation of high-frequency signals from the DC control circuit.

A total of 11 PIN diodes are integrated in the antenna. These diodes can be divided into five groups, among which D1, D2 and D3 are group A, D4 and D5 are group B, D6 and D7 are group C, D8 and D9 are group D, and D10 and D11 are group E. Group A PIN diodes are vertically embedded in the dielectric substrate to connect the lower rectangular monopole subunit and the top microstrip patch. The antenna can be operated in different modes by controlling the on/off state of the five groups of PIN diodes.

## 3. Working principle analysis

The three groups of PIN diodes A, B, and C are mainly used to control the working mode and frequency of the antenna, and the two groups of diodes D and E are used to control the pattern of the microstrip patch mode. The different frequency modes corresponding to the combinations of different states of the three groups of switches A, B and C are given in Table 1 and Figure 2.

Table 1. Frequency reconfigurable state table

Reconstruction state	Group A	Group B	Group C	Operating mode
State 1	ON	OFF		2.4GHz Single frequency antenna
State 2	OFF	ON	ON	5.2GHz Dual frequency antenna
State 3	OFF	ON	OFF	5.8GHz Dual frequency antenna

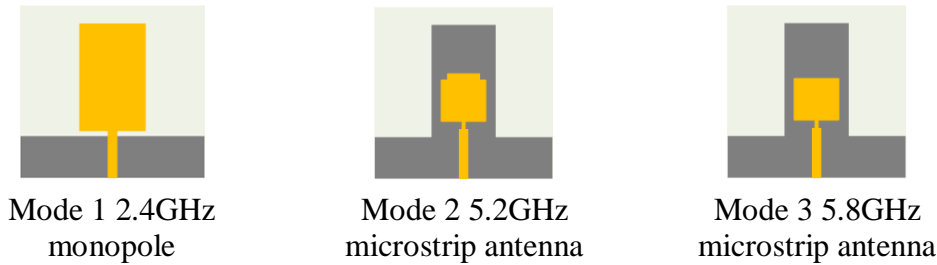


Fig. 2 Schematic diagram of the equivalent structure of each mode of the antenna.

When the antenna is in the microstrip patch mode, the reconfiguration of the pattern with directional radiation characteristics can be achieved through the combination of the different states of the D and E switches. The specific status is given in Table 2 and Figure 3.+

Table 2. Pattern Reconfigurable State Table

Reconstruction state	Group D	Group E	Operating mode	Reconstruction state
State A	OFF	ON	Reflection left	State A
State B	OFF	OFF	Default state	State B
State C	ON	OFF	Reflect right	State C

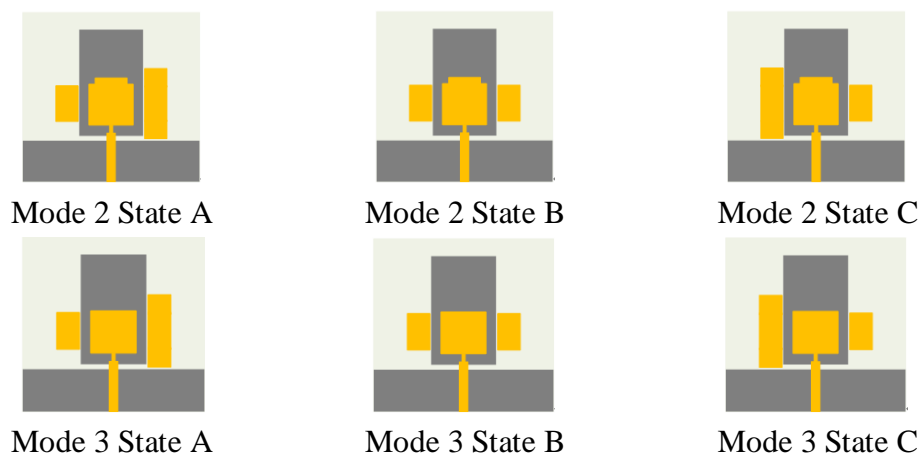


Fig. 3 Schematic diagram of pattern reconstruction in microstrip patch mode.

The specific working principle of the antenna is as follows: When the diodes of group A are turned on, the diodes of group B are turned off, and the state of the diodes of group C is arbitrary, the current of the antenna feeder can directly pass from the microstrip patch on the top layer through the PIN diodes of the group A in the conductive state. Directly flow into the rectangular monopole unit on the bottom layer, and the antenna works in 2.4GHz monopole mode with omnidirectional radiation; When the diodes of group A are turned off and the diodes of group B are turned on, the bottom rectangular monopole subunit is connected to the metal ground and directly serves as the ground plane of the microstrip patch unit. At this time, the antenna works on the directional radiation 5GHz microstrip patch. Film mode. In this mode, the resonant frequency of the microstrip patch antenna can be switched between 5.2GHz and 5.8GHz by controlling the on-off state of the C group PIN

diode; In addition, when the antenna is working in the 5GHz microstrip patch mode, the effective length of the symmetrically distributed metal sheets on both sides of the microstrip patch unit can be changed by controlling the D and E two sets of PIN diodes, so that they can be used as reflectors or guides. Directional device, so as to realize the reconfigurable pattern of the directional radiation microstrip patch antenna.

The surface current of the antenna under different modes is simulated and analyzed, and the simulation results are shown in Figure 4. It can be seen from the figure that when working in mode 1, the antenna surface current at 2.4GHz is mainly distributed on the rectangular monopole on the bottom layer, while there is almost no current distribution on the microstrip patch unit on the top layer; When working in mode 2, the antenna surface current at 5.2GHz is mainly distributed on the entire microstrip patch on the top layer (due to the conduction of group C diodes, the two microstrip patches form a whole), and the monopole unit on the bottom There is almost no current distribution; When working in mode 3, at 5.8GHz, the antenna current is mainly distributed on the microstrip patch on the bottom half of the top layer (due to the disconnection of the diodes in group C, only the microstrip patch connected to the feeder is effective), and on the bottom layer There is almost no current distribution on the monopole unit. The simulation result of the current distribution on the antenna surface well proves the correctness of the previous analysis of the antenna structure.

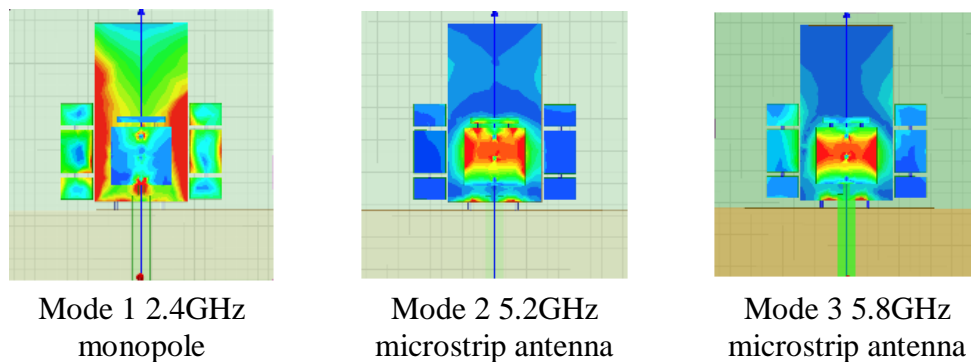


Fig. 4 Surface current distribution of each mode of antenna.

#### 4. Antenna simulation and test results analysis

The electromagnetic simulation software HFSS 13.0 is used to optimize and analyze the antenna parameters, and the final values of each size parameter of the antenna are shown in Table 3. Where L is the length of the entire dielectric plate.

Table 3. Antenna size parameter

Parameter	Value/mm	Parameter	Value/mm	Parameter	Value/mm
W	50	W1	3.4	W2	1.2
W3	11.5	W4	9	W5	17.6
W6	6	L	50	Lg	13
G1	1.5	L1	10.7	L2	1.1
L3	4	L4	8	L5	33
L6	15.6	L7	2		

After the final size is determined, the antenna is simulated and analyzed as follows, and the antenna is tested (the antenna test is completed on the Agilent E5071C).

##### 4.1 Work mode 1 result analysis

It can be seen from Figure 5 that the frequency range of  $S_{11} \leq -10\text{dB}$  of the antenna in this mode is 1.82GHz~3.07GHz, and the relative bandwidth is as high as 51.1%, which has good broadband

characteristics. The value of S11 at the resonance frequency is -30.25dB, which has a high degree of impedance matching. The frequency range of the VSWR 2 of the antenna is 1.81GHz~3.09GHz, which is consistent with the frequency range obtained by the S11 curve. In addition, comparing the simulated and measured curves shows that the two are basically consistent.

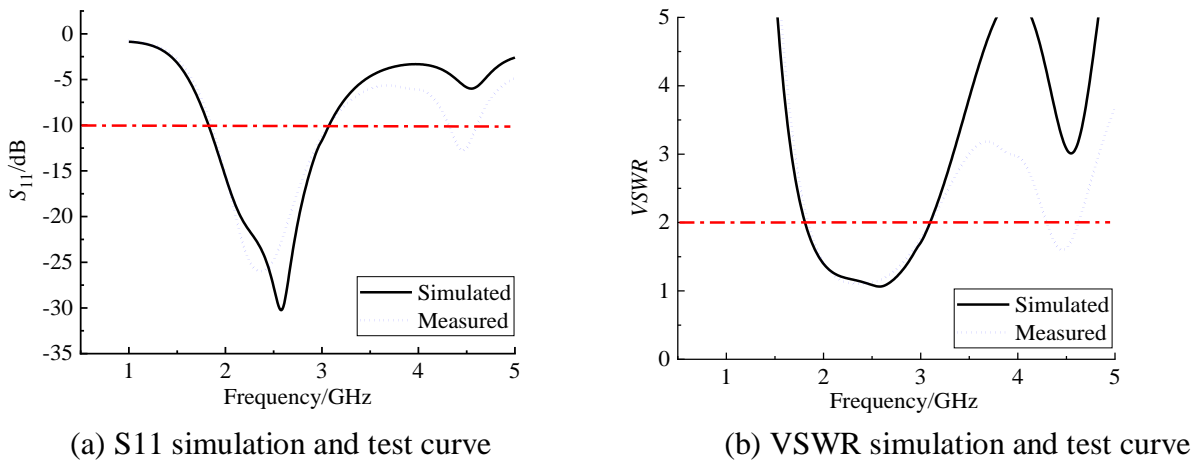


Fig. 5 S11 and VSWR simulation and test curves under the mode

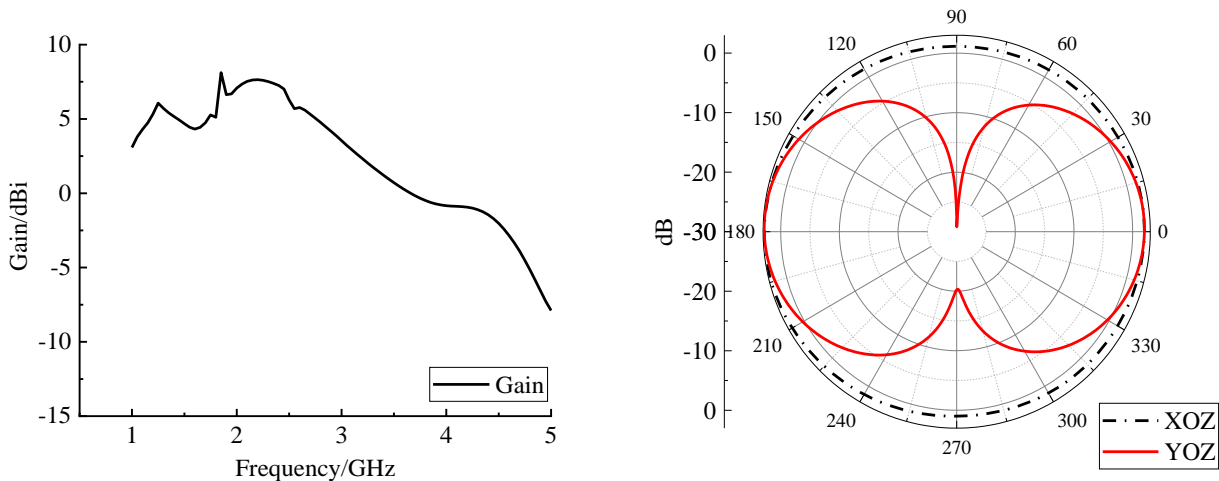


Fig. 6 Mode 1 gain curve simulation diagram

Fig. 7 Mode 1 radiation pattern

It can be seen from Fig. 6 that within the effective bandwidth of the antenna, the gain value varies from 3.09dBi to 8.12dBi, which has a higher gain. It can be seen from Figure 7 that the antenna has good directivity on the XOZ plane (E plane), the gain curve is circular, the gain values are all greater than 0dBi, and the peak gain is 2.78dBi. On the YOZ plane (H plane), the shape of the gain curve of the antenna is similar to the "8" shape, the gain is poor in the angle range of 75°~105° and 255°~285°, and distortion occurs at 90° and 270°, The gain reaches the lowest value, respectively -28.67dBi and -20.33dBi, and the gain characteristic is good in the other directions, the peak gain point coincides with the XOZ surface, and has a higher gain value. To sum up, when the antenna is working in mode 1, the gain curve exhibits better omnidirectionality and a larger gain value in the entire XOZ plane. Although there is distortion in individual directions on the YOZ plane, in general, Good gain and directivity, with omnidirectional radiation characteristics.

**4.2 Work mode 2 result analysis**

It can be seen from Figure 8 that the frequency range of the antenna's S11 below -10dB in this mode is 5.05GHz~5.43GHz, and the relative bandwidth is 7.3%, which can completely cover the 5.2GHz

frequency band of WLAN and has better bandwidth characteristics. In addition, the value of  $S_{11}$  at the resonant frequency point is  $-35.22\text{dB}$ , and the impedance matching degree is relatively high; the frequency range of the VSWR 2 of the antenna is  $5.04\text{GHz}\sim 5.44\text{GHz}$ , which is consistent with the frequency range obtained by the  $S_{11}$  curve. The comparison shows that the measured curve and the simulated curve are in good agreement.

Fig. 9 is a curve simulation diagram of the antenna gain varying with frequency at a point in the time space of mode 2 when the antenna works. It can be seen from the figure that within the effective frequency band of the antenna, the gain value varies from  $1.64\text{dBi}$  to  $2.97\text{dBi}$ , which has good gain characteristics.

Figure 10 shows three different reconfigurable directional patterns when the antenna works in mode 2. From the previous analysis of the antenna structure, it can be known that when the antenna is working in mode 2, the directional pattern can be switched between three different states by controlling the D and E PIN diodes. Figure 10(a) is the radiation pattern of the antenna in the default state (both groups of PIN diodes are in the off state). It can be seen from the figure that the gain curve of the antenna on the XOZ plane (E plane) mainly has good gain characteristics in the continuous angular direction of  $250^\circ\sim 360^\circ$  and  $0^\circ\sim 20^\circ$ , and the gain value is greater than  $0\text{dBi}$ . , And the peak gain is  $3.32\text{dBi}$ , and in the other directions except for the  $80^\circ\sim 110^\circ$  direction, the gain is greater than  $0\text{dBi}$ , the other directions are all less than  $0\text{dBi}$ , so the antenna exhibits directional radiation characteristics on the XOY plane. The gain curve on the YOZ plane (H plane) is greater than  $0\text{dBi}$  in the direction of  $180^\circ\sim 240^\circ$ , and the peak gain is  $1.63\text{dBi}$ , while the gain characteristics in the other directions are poor, and they also exhibit directional radiation characteristics.

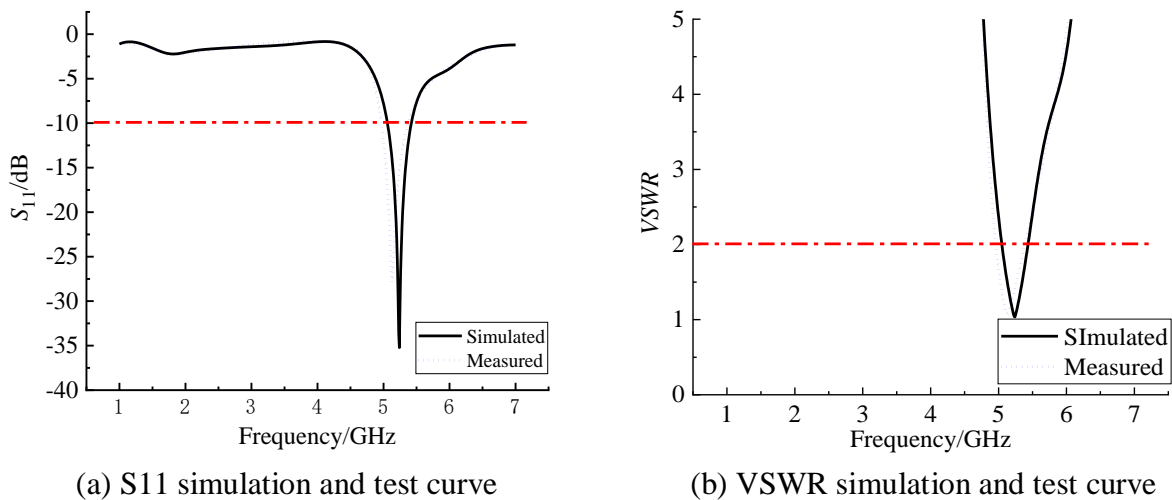


Fig. 8.  $S_{11}$  and VSWR simulation and test curves in mode 2

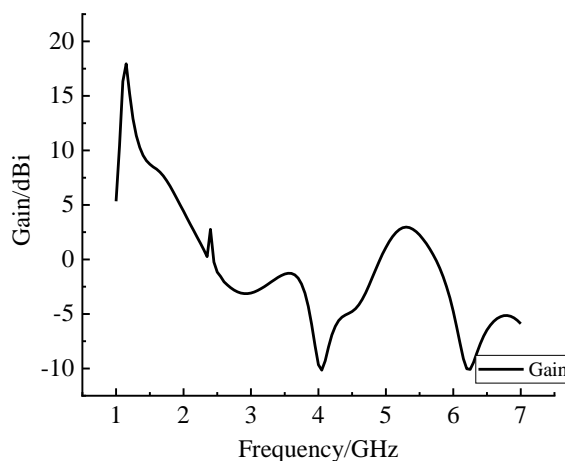


Fig. 9. Simulation diagram of gain curve in mode 2

When the diodes of group D are turned off and the diodes of group E are turned on, since the effective length of the right metal sheet is longer than the microstrip patch, it acts as a reflector, while the left metal sheet acts as a reflector because the effective length is less than the microstrip patch. The role of the director. The radiation pattern at this time is shown in Figure 10(b). It can be seen from the figure that the radiation pattern of the antenna in this state also exhibits directional radiation characteristics on both the XOZ plane and the YOZ plane. The YOZ plane is not much different from the default state, while on the XOZ plane, the gain is greater than the 0dBi direction range. The clockwise rotation becomes  $225^{\circ}\sim 360^{\circ}$ , and the peak gain is 3.71dBi. When the diodes of group D are turned on and the diodes of group E are turned off, the equivalent state of the metal sheets on both sides of the microstrip patch becomes the reflector on the left and the director on the right. The radiation pattern at this time is shown in Figure 10. (c) Shown. It can be seen from the figure that the directional pattern on the YOZ plane is still basically the same as the default state, while on the XOZ plane, the direction range of the gain greater than 0dBi produces a counterclockwise rotation to  $330^{\circ}\sim 360^{\circ}$  and  $0^{\circ}\sim 120^{\circ}$ , a total of  $150^{\circ}$  Continuous angle range, peak gain is 3.13dBi.

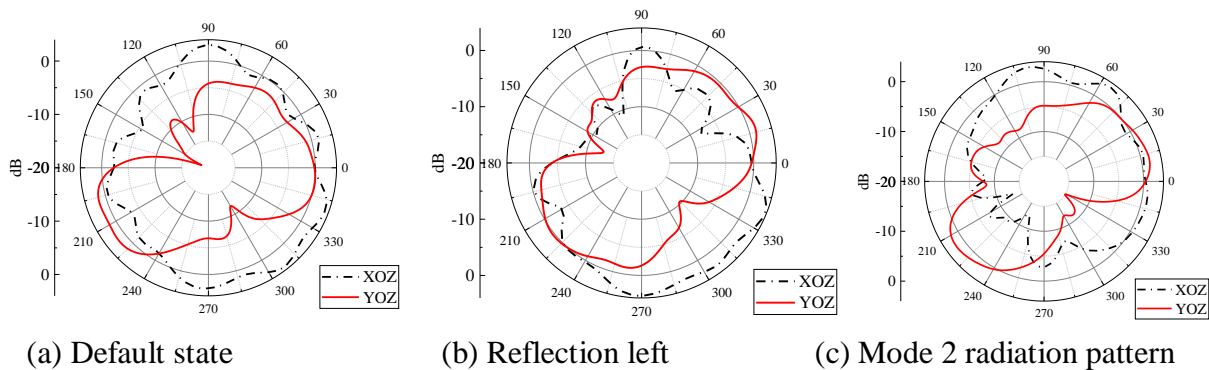


Fig. 10 Different pattern states in mode 2

### 4.3 Work mode 3 result analysis

It can be seen from Figure 11 that the frequency range of the antenna's S11 below -10dB is 5.51GHz~6.03GHz, and the relative bandwidth is 9.0%. It can completely cover the 5.8GHz frequency band of WLAN and has good bandwidth characteristics. In addition, the value of S11 at the resonance frequency point is -32.28dB, which has good impedance matching characteristics; the frequency range of the antenna's VSWR 2 is 5.51GHz~6.04GHz, which is basically the same as the frequency range obtained by the S11 curve. It can be seen from Figure 12 that in the effective frequency band of the antenna, its gain value varies from 1.32dBi to 4.67dBi, and it has better gain characteristics.

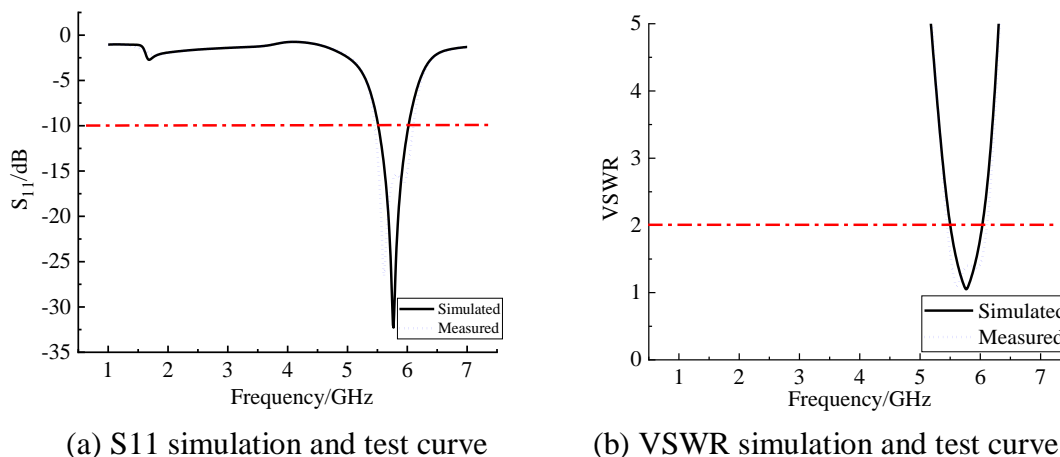


Fig. 11. Mode 3 S11 and VSWR simulation and test curves

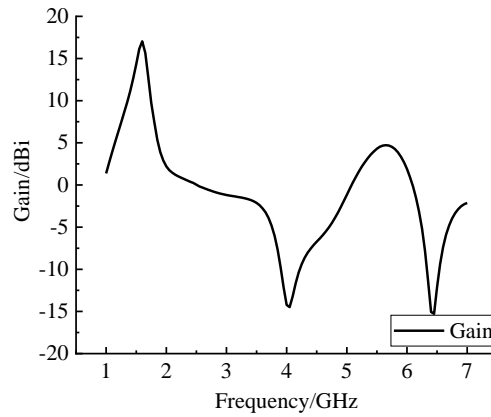


Fig. 12. Simulation diagram of gain curve in mode 3

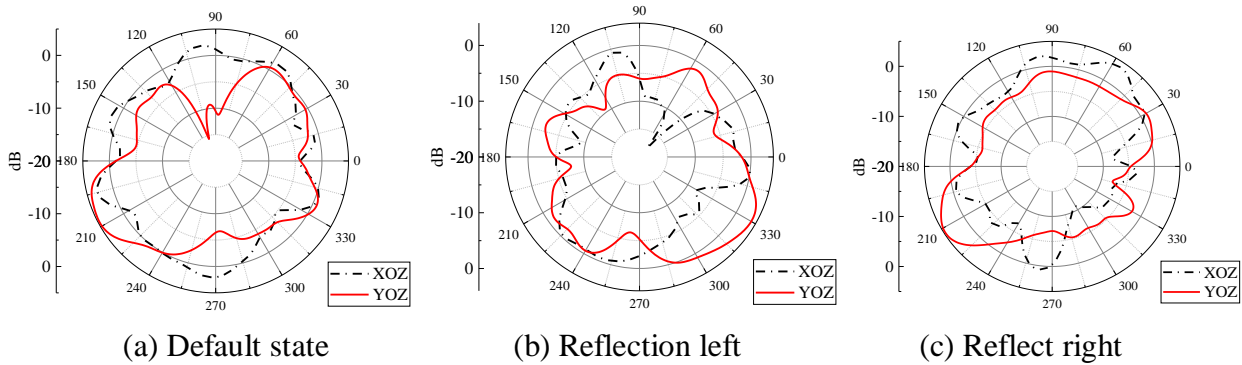


Fig. 13. Different pattern states in mode three

Figure 13 shows three different reconfigurable directional patterns when the antenna works in mode 3. These three states can be achieved by controlling the on/off states of the D and E PIN diodes. Figure 13(a) is the radiation pattern of the antenna in the default state. It can be seen from the figure that the gain curve of the antenna on the XOZ plane (E plane) mainly has good gain characteristics in the angular range of  $40^{\circ}\sim 110^{\circ}$ ,  $140^{\circ}\sim 210^{\circ}$  and  $240^{\circ}\sim 290^{\circ}$ , and the peak gain is 1.97 respectively. dBi, 2.98dBi and 2.07dBi, and the gain characteristics in the other directions are poor. Therefore, the antenna exhibits directional radiation characteristics on the XOY surface. The gain curve on the YOZ plane (H plane) is greater than 0dBi in the direction of  $180^{\circ}\sim 240^{\circ}$ , and the peak gain reaches 4.73dBi, while the gain characteristic in the other directions is poor, and it also shows the directional radiation characteristic.

Same as mode 2, in mode 3, the effective length of the two sets of metal sheets symmetrically distributed on both sides of the top microstrip patch unit can be controlled by controlling the on or off states of the two sets of PIN diodes D and E. So that the metal sheets on both sides can be used as reflectors or guides. Figure 13(b) is the radiation pattern of the antenna at 5.8GHz with the right side as the reflector and the left side as the director. It can be seen from the figure that the antenna also exhibits directional radiation characteristics on both XOZ and YOZ planes. The main radiation direction on the XOZ plane is  $220^{\circ}\sim 260^{\circ}$ , and the main radiation direction on the YOZ plane is  $280^{\circ}\sim 350^{\circ}$ , and It has a maximum gain of 3.13dBi. Figure 13(c) is the radiation pattern of the antenna when the left side is the reflector and the right side is the director. It can be seen from the figure that the antenna is directional radiation on both planes, and the main radiation direction on the XOZ plane becomes  $25^{\circ}\sim 115^{\circ}$  with a maximum gain of 3.89dBi, while the main radiation direction on the YOZ plane is  $185^{\circ}\sim 230^{\circ}$  with a maximum gain of 4.74dBi.

In order to illustrate the performance of the antenna designed in this paper more intuitively, the antennas in literature [6] and literature [7] are selected to compare several important indicators. Table 4 gives specific comparison data. It can be seen that the antenna designed in this paper can achieve larger gain, larger bandwidth and more reconfigurable states in a similar or smaller size.

## 5. Conclusions

This paper designs a reconfigurable antenna with a hybrid frequency and pattern. This antenna can switch between three modes and a total of seven states, and achieve complete coverage of the WLAN frequency band. The antenna has better broadband characteristics and higher gain in each mode and state, and has good impedance matching characteristics. For directivity, this antenna has 2.4GHz omnidirectional radiation characteristics, and in 5.2GHz and 5.8GHz directional radiation modes, the pattern reconstruction also has a larger beam scanning range, which meets the design goals proposed in the previous article Requirements, the design methods and ideas used in this design can also provide a certain reference value for the design of other frequency and pattern hybrid reconfigurable antennas.

Table 4. Performance comparison table

Frequency and pattern hybrid reconfigurable antenna	Resonance frequency	Relative bandwidth	Maximum gain	Number of reconfigurable states	Number of switches	Area (mm <sup>2</sup> )
Reference [6]	4.45~4.54Ghz	2.2%	3.00dBi	7	6	50*50
	4.74~4.86Ghz	2.3%	3.50dBi			
	5.14~5.26Ghz	2.4%	3.70dBi			
	5.69~5.90Ghz	3.5%	4.00dBi			
Reference [7]	2.21~2.90Ghz	27.0%	0.70dBi	3	5	80*32
	5.26~5.56Ghz	5.5%	2.50dBi			
	5.27~5.89Ghz	11.1%	2.80dBi			
This design	1.82~3.07Ghz	51.1%	2.78dBi	7	11	50*50
	5.05~5.43Ghz	7.3%	3.71dBi			
	5.51~6.03Ghz	9.0%	4.73dBi			

## References

- [1] Li Tong, Zhai Huiqing, Wang Xin, et al. Frequency-reconfigurable bow-tie antenna for bluetooth, WiMAX, and WLAN applications[J]. IEEE Antennas and Wireless Propagation Letters, 2015, 14: 171-174.
- [2] Chen Shulin, Wei Feng, Qin Peiyuan, et al. A multi-linear polarization reconfigurable unidirectional patch antenna[J]. IEEE Transactions on Antennas and Propagation, 2017, 65(8): 4299-4304.
- [3] Ni Chun, Chen Mingsheng, Zhang Zhongxiang, et al. Design of frequency-and polarization-reconfigurable antenna based on the polarization conversion metasurface[J]. IEEE Antennas and Wireless Propagation Letters, 2018, 17(1): 78-81.
- [4] Nguyen-Trong N, Piotrowski A, Hall L, et al. A frequency- and polarization-reconfigurable circular cavity antenna[J]. IEEE Antennas and Wireless Propagation Letters, 2017, 16: 999-1002.
- [5] Liu Jie, Li Jianying, Xu Rui. Design of very simple frequency and polarisation reconfigurable antenna with finite ground structure[J]. Electronics Letters, 2018, 54(4): 187-188.
- [6] Selvam Y P, Kanagasabai M, Alsath M G N, et al. A low profile frequency and pattern reconfigurable antenna[J]. IEEE Antennas and Wireless Propagation Letters, 2017, 16: 3047-3050.
- [7] Li Pengkai, Shao Zhenhai, Wang Quan, et al. Frequency- and pattern-reconfigurable antenna for multistandard wireless applications[J]. IEEE Antennas
- [8] Ge Lei, Li Yujian, Wang Jianpeng, et al. A low-profile reconfigurable cavity-backed slot antenna with frequency, polarization, and radiation pattern agility[J]. IEEE Transactions on Antennas and Propagation, 2017, 65(5): 2182-2189.
- [9] Selvam Y P, Elumalai L, Alsath M G N, et al. A novel frequency and pattern reconfigurable rhombic patch antenna with switchable polarization[J]. IEEE Antennas and Wireless Propagation Letters, 2017, 16: 1639-1642.